Electroelastic analysis of four mode-III cracks originating from a circular hole in piezoelectric materials

JunHong Guo[1,*], ZiXing Lu[2], Jing Yu[1]

[1] College of Science, Inner Mongolia University of Technology, Hohhot 010051, China
[2] Institute of Solid mechanics, Beihang University, Beijing 100191, China
* Corresponding author: jhguo@imut.edu.cn

Abstract The fracture behavior of four non-symmetric radial cracks originating from a circular hole in piezoelectric materials subjected to remotely uniform in-plane electric loading and anti-plane mechanical loading is studied in this paper. The problem is transformed using the complex variable method and the technique of conformal mapping into Cauchy integral equations. To solve the Cauchy integral equations, the analytical solutions of the stress and the electric displacement intensity factors, energy release rate and mechanical strain energy release rate are obtained under the electrically impermeable and electrically permeable assumptions, respectively. Several known results are the special cases of the present results and new models used for simulating more practical defects in piezoelectric materials are derived as well, such as three radial cracks originating from a circular hole, semi-circular hole with an edge crack originating from a semi-infinite plane and a semi-infinite plane with an edge crack. Numerical examples are provided graphically to show the effects of the geometrical parameters on the energy release rate and the mechanical strain energy release rate.

Keywords Piezoelectric materials, Circular hole, Edge cracks, mapping function, Analytical solution

1. Introduction

Due to their intrinsic electromechanical coupling phenomenon, piezoelectric materials have been widely used as transducer and sensor in smart structures and devices. However, one inherent weakness of piezoelectric ceramics is the brittleness in mechanical behavior. When subjected to mechanical and electric loading in service, the stress concentrations can induce crack initiation and propagation, which will lead to the failure of these piezoelectric materials. Therefore, it is of great importance to analyze the fracture behavior of piezoelectric materials, especially when cracks emanating from holes are involved.

In recent years, the crack problems of piezoelectric materials have received considerable attention under anti-plane shear loading due to the practical importance [1-6]. In fact, there exist many kinds of complicated configurations during manufacture and service of the holed structures, e.g., cracks originating from circular hole, semi-circular hole with an edge crack originating from a semi-infinite solid, T-shaped crack, cross-shaped crack, etc. Recently, Wang and Gao [7] solved the two symmetrical cracks and a single crack originating from the edge of a circular hole in a piezoelectric solid by introducing mapping fucntion, and presented the exact solutions of the field intensity factors and the energy release rate. By developing new mapping functions, Guo et al. [8,9] investigated the two asymmetrical edge cracks emanating from an elliptical hole in a piezoelectric material under the electrically impermeable and the electrically permeable boundary conditions, respectively, and obtained the exact solutions of the field intensity factors and the energy release rate. To ours' knowledge, the existing research is focused on the collinear cracks parallel to the x-axis originating from holes. For an occurrence of the cracks parallel to y-axis direction originating from holes, however, the corresponding research is very lacking in a piezoelectric solid, which may have the surprise results. Thus, it is practical and necessary to study the fracture behavior of four

non-symmetrical radial cracks at the edge of a circular hole. Furthermore, it is very challenging and meaningful to present the analytical solutions for the complicated crack problems, since these solutions can provide the theoretical analysis for fracture problems in piezoelectric materials, and can also serve as a benchmark for the purpose of judging the accuracy and efficiency of various numerical and approximate methods.

In this paper, we study the anti-plane problem of four non-symmetrical radial cracks at the edge of a circular hole in a transversely isotropic piezoelectric solid based on two kinds of electric boundary conditions, i.e., the electrically impermeable and the electrically permeable. A new conformal mapping is developed to reduce the problem to the solution of Cauchy integral equation. In addition, the analytical solutions of the field intensity factors, the energy release rate (ERR) and the mechanical strain energy release rate (MSERE) are derived. It is seen that the stress intensity factors of some special cases derived from the present results agree well with the corresponding results of the pure elastic materials.

2. Basic formulation

In a rectangular coordinate system $x_i (i = 1, 2, 3)$, consider a transversely isotropic piezoelectric solid with the poling direction along the positive x_3 axis and the isotropic plane in the $x_1 - x_2$ plane. The constitutive equation for a linear piezoelectric media can be given as

$$[s_{3i}, D_i]^{\mathrm{T}} = \mathbf{B}_0 [g_{3i}, -E_i]^{\mathrm{T}} \tag{1}$$

where i=1, 2, T denotes a transpose of a matrix, and

$$\mathbf{B}_0 = \begin{matrix} 矩 \\ 阵 \\ 省 \\ 略 \\ 掉 \\ 的 \\ 内 \\ 容 \end{matrix} \begin{matrix} c_{44} & e_{15} \\ e_{15} & -\varepsilon_{11} \end{matrix} \tag{2}$$

where c_{44}, e_{15} and ε_{11} are the elastic constant, the piezoelectric constant and the dielectric permittivity, respectively.

The generalized strain-displacement relations have the form

$$g_{3i} = w_{,i}, \quad E_i = -\varphi_{,i} \tag{3}$$

where a comma in the subscripts stands for a partial differentiation.

The equilibrium equation and the charge conservation equation, in the absence of the body force and electric charge densities, can be written as

$$s_{3i,i} = 0, \quad D_{i,i} = 0 \tag{4}$$

Substituting Eqs. (1) and (2) into Eq. (4), we have

$$\nabla^2 w = 0, \quad \nabla^2 \varphi = 0 \tag{5}$$

The general solution of Eq. (5) can be expressed by the analytical function $\mathbf{f}(z)$ [4]

$$\mathbf{u} = \mathbf{A}\mathbf{f}(z) + \overline{\mathbf{A}\mathbf{f}(z)}, \quad \mathbf{u} = (w, \varphi)^{\mathrm{T}} \tag{6}$$

where $z = x_1 + \mathrm{i}x_2$. Thus, the stress and electric displacement can be expressed as

$$[s_{31} - \mathrm{i}s_{31}, D_1 - \mathrm{i}D_2]^{\mathrm{T}} = \mathbf{B}_0[g_{31} - \mathrm{i}g_{32}, -E_1 + \mathrm{i}E_2]^{\mathrm{T}} = \mathbf{B}_0\mathbf{f}'(z) \tag{7}$$

Let we introduce a potential function ϕ, such that

$$[s_{31}, D_1]^{\mathrm{T}} = -\mathbf{f}_{,2}, \quad [s_{32}, D_2]^{\mathrm{T}} = \mathbf{f}_{,1} \tag{8}$$

From Eqs. (7) and (8), one finds

$$\mathbf{f}'(z) = \mathbf{B}\mathbf{f}(z) \tag{9}$$

where $\mathbf{A}$ and $\mathbf{B}$ stand for the material constant matrices defined as

$$\mathbf{A} = \mathbf{I}, \quad \mathbf{B} = \mathrm{i}\mathbf{B}_0 \tag{10}$$

where $\mathbf{I}$ is a 2×2 unit matrix.

The boundary conditions along the surfaces of crack and circular hole can be written as

$$\int_s [t_3, D_n]^{\mathrm{T}}\,\mathrm{d}s = -\int_s [s_{32}\mathrm{d}x_1 - s_{31}\mathrm{d}x_2, D_2\mathrm{d}x_1 - D_1\mathrm{d}x_2]^{\mathrm{T}}\,\mathrm{d}s = -\,\mathrm{Re}\int_s \mathrm{d}\mathbf{f} = \mathrm{Re}[\mathbf{B}\mathbf{f}(z)] \tag{11}$$

where t_3 and D_n represent the anti-plane shear traction and the normal component of electric displacement along the boundary.

3. Mapping function and field intensity factors

Consider four non-symmetrical radial cracks at the edge of a circular hole in an infinite piezoelectric solid, as shown in Fig. 1. Using the technique of conformal mapping and complex variable method, we study the complex potentials, the field intensity factors, ERR and MSERR under two different electric boundary conditions as follows.

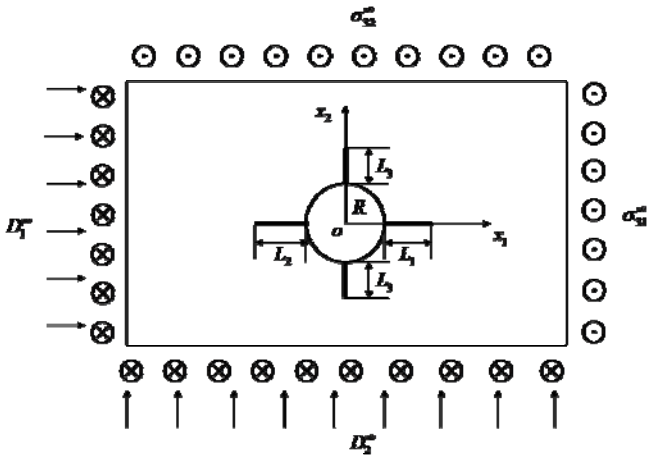

Fig. 1. Four non-symmetrical radial cracks at the edge of a circular hole in an infinite piezoelectric solid

In this case, the potential vector has the form (Zhang and Gao [6])

$$\mathbf{f}(z) = \mathbf{c}^{\infty} z + \mathbf{f}_0(z) \tag{12}$$

where $\mathbf{c}^{\infty}$ is a complex constant related to the remote loading conditions, and $\mathbf{f}_0(z)$ is an

unknown complex function that nulls at infinity, i.e., $\mathbf{f}_0(\infty)=\mathbf{0}$.

When the piezoelectric solid is subjected to uniform remote out-plane shear and in-plane electric field loadings, i.e., $\boldsymbol{\Sigma}_{2\infty}=[\sigma_{32}^{\infty},D_2^{\infty}]^{\mathrm{T}}$ and $\boldsymbol{\Sigma}_{1\infty}=[\sigma_{31}^{\infty},D_1^{\infty}]^{\mathrm{T}}$, the complex constant vector $\mathbf{c}^{¥}$ in Eq. (12) can be determined as

$$\mathbf{c}^{?}=\mathbf{B}^{1}[s_{31}^{\prime\prime}-\mathrm{i}s_{32},D_1^{\prime\prime}-\mathrm{i}D_2]^{\mathrm{T}} \tag{13}$$

In this study, two kinds of electric crack surface conditions are examined, i.e., electrically impermeable and permeable. For simplicity, they are identically expressed as

$$[s_{32},D_2]^{\mathrm{T}}=\text{矯}D_2^0]^{\mathrm{T}} \tag{14}$$

For the electrically impermeable case, $D_2^0=0$, whereas for the electrically permeable case, D_2^0 is unknown to be determined from the potential function continuity conditions along the surfaces of cracks and hole

$$\boldsymbol{\phi}^{+}=\boldsymbol{\phi}^{-},\ \varphi^{+}=\varphi^{-} \tag{15}$$

where superscript + and – denote the potential functions inside and outside the cracks and hole, respectively.

3.1. Electrically impermeable case

If the crack length is shorter than the hole-size, and the electric field inside the hole is smaller, the assumption of impermeable electric boundary condition is more reasonable. Thus, noting Eq. (13), Eq. (12) can be reduced to

$$\mathbf{B}\mathbf{f}_0(z)+\overline{\mathbf{B}\mathbf{f}_0(z)}=-(\mathbf{B}\mathbf{c}^{\infty}z+\overline{\mathbf{B}\mathbf{c}^{\infty}z}) \tag{16}$$

We develop a new mapping function as follows

$$z=\omega(\zeta)=\frac{R}{4\zeta}\left\{\sqrt{\left[f(\zeta+1)^2+g(\zeta-1)^2\right]^2-16a^2\zeta^2}+\sqrt{\left[f(\zeta+1)^2+g(\zeta-1)^2\right]^2-16(a^2+1)\zeta^2}\right\} \tag{17}$$

where

$$\begin{aligned}&f=\sqrt{a^2+c^2},\quad g=\sqrt{a^2+b^2}\\ &a=\frac{1}{2}\left(\frac{R+L_3}{R}-\frac{R}{R+L_3}\right),\quad b=\frac{1}{2}\left(\frac{R+L_2}{R}+\frac{R}{R+L_2}\right),\quad c=\frac{1}{2}\left(\frac{R+L_1}{R}+\frac{R}{R+L_1}\right)\end{aligned} \tag{18}$$

It can be shown that Eq. (17) provides a mapping function from the outside region of the circular hole and cracks to the interior of a unit circle in the ζ-plane, and $z=R+L_1=\omega(1)$.

In the ζ-plane, Eq. (16) can be transformed into

$$\mathbf{B}\mathbf{f}_0(\sigma)+\overline{\mathbf{B}\mathbf{f}_0(\sigma)}=-\left[\mathbf{B}\mathbf{c}^{\infty}\omega(\sigma)+\overline{\mathbf{B}\mathbf{c}^{\infty}}\,\overline{\omega(\sigma)}\right] \tag{19}$$

where σ is the point on the unit circle, and $\mathbf{f}_0(\sigma) = \mathbf{f}_0(\omega(\sigma))$ is defined.

Taking Cauchy integrals $\frac{1}{2\pi \mathrm{i}}\int_\gamma \frac{d\sigma}{\sigma-\zeta}$ at the two sides of Eq. (19), we obtain

$$\mathbf{B}\mathbf{F}_0(\zeta) = -\boldsymbol{\phi}_{,1}^{\infty}\left[\omega'(\zeta) + \frac{R(f+g)}{2\zeta^2}\right] \tag{20}$$

The vector of field intensity factors can be expressed in the ζ-plane, as [8]

$$\boldsymbol{k} = (k_\sigma, k_D)^{\mathrm{T}} = 2\sqrt{\pi}\lim_{\zeta\to 1}\frac{\mathbf{B}\mathbf{F}_0(\zeta)}{\sqrt{\omega''(\zeta)}} \tag{21}$$

Substituting Eqs. (17) and (20) into Eq. (21), one finally has

$$\boldsymbol{k}_{\mathrm{imp}} = \sqrt{\pi L_1}\begin{pmatrix}\sigma_{32}^{\infty}\\ D_2^{\infty}\end{pmatrix}K \tag{22}$$

where K called the dimensionless intensity factor is defined as

$$K = \sqrt{\frac{2Rc(f+g)\sqrt{c^2-1}}{L_1 f\left(c+\sqrt{c^2-1}\right)}} \tag{23}$$

3.2. Electrically permeable case

According to the method of Guo et al. [9], the potential functions inside the cracks and hole can be expressed as

$$\boldsymbol{\phi}^{+} = (D_2^0 x_1 - D_1^0 x_2)\mathbf{i}_2, \tag{24}$$

$$\varphi^{+} = -E_1^0 x_1 - E_2^0 x_2, \tag{25}$$

where $\mathbf{i}_2 = [0,1]^{\mathrm{T}}$, and D_k^0 and E_k^0 are the components of the electric displacement and electric field inside the elliptical hole and the cracks, respectively, which are constant and to be determined by the loading condition.

The potential functions outside the cracks and hole can be expressed as

$$\boldsymbol{\phi}^{-} = \boldsymbol{\Sigma}_{2\infty} x_1 - \boldsymbol{\Sigma}_{1\infty} x_2 + 2\mathrm{Re}[\mathbf{k}_0(z)], \tag{26}$$

$$\varphi^{-} = -E_1^{\infty} x_1 - E_2^{\infty} x_2 + 2\mathrm{Im}[\mathbf{Y}\mathbf{k}_0(z)]_2, \tag{27}$$

where $\mathbf{k}_0(z) = \mathbf{B}\mathbf{f}_0(z)$, $\mathbf{Y} = \mathrm{i}\mathbf{A}\mathbf{B}^{-1}$.

Substituting Eqs. (24)-(27) into Eq. (15), we get

$$\mathbf{BF}_0(\zeta) = \frac{(a+b)(\varepsilon_1+\varepsilon_2)}{4\zeta^2}\mathbf{\Sigma}^{2\infty}, \tag{28}$$

$$D_2^0 = D_2^\infty - \frac{e_{15}}{c_{44}}\sigma_{32}^\infty. \tag{29}$$

where $\mathbf{\Sigma}^{2\infty} = [\sigma_{32}^\infty, D_2^\infty - D_2^0]^{\mathrm{T}}$.

Substituting Eqs. (28) and (29) into Eq. (21), one finally has

$$\boldsymbol{k}_{\mathrm{per}} = \sqrt{\pi L_1}\begin{pmatrix}\sigma_{32}^\infty \\ D_2^\infty - D_2^0\end{pmatrix}K \tag{30}$$

The dimensionless intensity factor K can be used to determine the field intensity factors and the ERR of four non-symmetrical radial cracks at the edge of a circular hole. In some limiting special cases, the known results [7-12] are the special cases of the present solutions. Furthermore, new configurations such as three radial cracks originating from a circular hole, semi-circular hole with an edge crack originating from a semi-infinite plane and a semi-infinite plane with an edge crack can be simulated from the present results.

4. Energy release rate

As mentioned above, the stress intensity factors (SIFs) and the electric displacement intensity factors (EDIFs) are independent and they are only related to the corresponding mechanical and electrical loading for the electrically impermeable boundary condition. For the electrically permeable case, both the SIFs and the EDIFs are independent on the electrical loading at infinity. So the SIFs and EDIFs can not perfectly describe the fracture characteristics of piezoelectric materials. In this study, the ERR and the MSERR are chosen as the fracture criterion to analyze the fracture behavior of four cracks emanating from a circular hole in piezoelectric materials.

The computational expressions of the ERR and the MSERR can be written as the following forms, respectively

$$G = \frac{1}{2}\boldsymbol{k}^{\mathrm{T}}\mathbf{B}_0^{-1}\boldsymbol{k} \tag{31}$$

$$G^M = \frac{1}{2}k_\sigma k_\gamma, \tag{32}$$

where

$$k_\gamma = \frac{e_{15}k_D + \varepsilon_{11}k_\sigma}{e_{15}^2 + \varepsilon_{11}c_{44}}. \tag{33}$$

Substituting Eqs. (2), (22) and (30) into Eq. (31), the ERR for the electrically impermeable and the electrically permeable cases are obtained, respectively

$$G_{\mathrm{imp}} = \frac{\pi L_1 K^2}{2(e_{15}^2 + \varepsilon_{11}c_{44})}\left(\varepsilon_{11}\sigma_{32}^{\infty 2} + 2e_{15}\sigma_{32}^\infty D_2^\infty - c_{44}D_2^{\infty 2}\right) \tag{34}$$

$$G_{\text{per}} = \frac{\pi L_1 K^2}{2c_{44}} (\sigma_{32}^{\infty})^2 \tag{35}$$

It is seen that the ERR for the electrically impermeable case is dependent on the applied mechanical and electrical loadings at infinity, while it is only dependent on the applied mechanical loading at infinity for the electrically permeable one.

Substituting Eqs. (22), (30) and (33) into Eq. (32), the MSERR for the electrically impermeable and the electrically permeable cases are obtained, respectively

$$G_{\text{imp}}^{M} = \frac{\pi L_1 K^2}{2(e_{15}^2 + \varepsilon_{11} c_{44})} \left(\varepsilon_{11} \sigma_{32}^{\infty 2} + e_{15} \sigma_{32}^{\infty} D_2^{\infty} \right) \tag{36}$$

$$G_{\text{per}}^{M} = \frac{\pi L_1 K^2}{2c_{44}} (\sigma_{32}^{\infty})^2 \tag{37}$$

It is found that from Eq. (35) and (37), the MSERR is equal to the ERR for the electrically permeable boundary condition.

5. Numerical results

To illustrate the singular electro-elastic fields at the tip of crack, numerical examples for a cracked PZT-5H piezoelectric ceramic are given, material properties of which are [1] $c_{44} = 3.53 \times 10^{10}\ \text{N/m}^2$, $e_{15} = 17.0\,\text{C/m}^2$, $\varepsilon_{11} = 151 \times 10^{-10}\,\text{C/Vm}$ and $G_{\text{cr}} = 5.0\,\text{N/m}$, where G_{cr} is the critical energy release rate.

Figs. 2-4 show the variation of the normalized ERR with geometrical parameters for a fixed-size hole of $R = 0.01\text{m}$ under combined mechanical loading $\sigma_{32}^{\infty} = 6\,\text{MPa}$ and electric loading $D_2^{\infty} = 2\text{e}-3\,\text{C/m}^2$. It will be noted that the electrically permeable case gives the highest value of G/G_{cr}, while the electrically impermeable case yields the lowest value of G/G_{cr}. It is easily seen from Figs. 2 and 3 that an increase of the right and the left cracks length always enhances the crack growth. The same conclusion has been drawn in Refs. [7-9]. Fig. 4 shows the variation of G/G_{cr} with the perpendicular crack length L_3 for given the right crack length $L_1 = 0.005\,\text{m}$ and different values of the left crack length L_2. It is interesting to note that when the ratio of L_2/R equals to 0.5, i.e., $L_2 = L_1$, the normalized ERR at the tip of the right crack is not affected by the change of the perpendicular crack length. This conclusion is derived from the geometrical symmetry for the present model under the symmetrical loading conditions. For the other values of

L_2/R, there are following two trends: When the value of L_2/R is larger than 0.5, i.e., $L_2 > L_1$, the normalized ERR decreases with the ratio of L_3/R increasing. On the other hand, when the value of L_2/R is smaller than 0.5, i.e., $L_2 < L_1$, the normalized ERR increases as the ratio of L_3/R becomes large. The results show that if the length of left crack is larger than that of right crack, an increase of length of the perpendicular cracks can retard the crack growth. In contrast to that, if the length of left crack is smaller than that of right one, the increase of the length of the perpendicular cracks can enhance the crack propagation. These useful conclusions will provide the theoretical instruction on fracture analysis and structural design in engineering. In addition, the normalized ERR is close to constants as L_3/R tends to infinite, which corresponds to the case of semi-circular hole with an edge crack at the edge of semi-infinite solid.

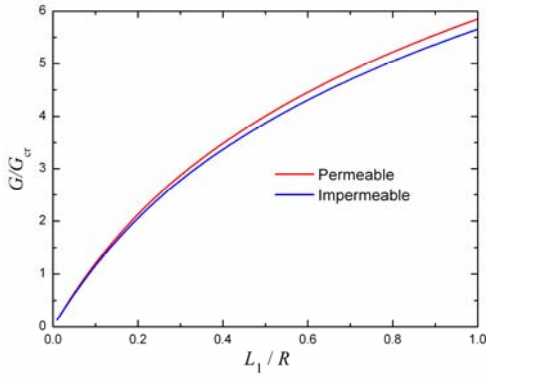

Fig. 2 Variation of G/G_{cr} with a ratio of L_1/R

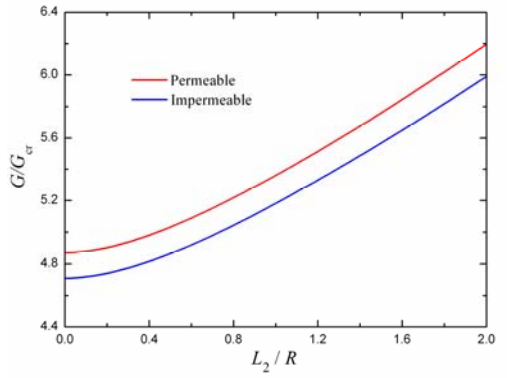

Fig. 3 Variation of G/G_{cr} with a ratio of L_2/R

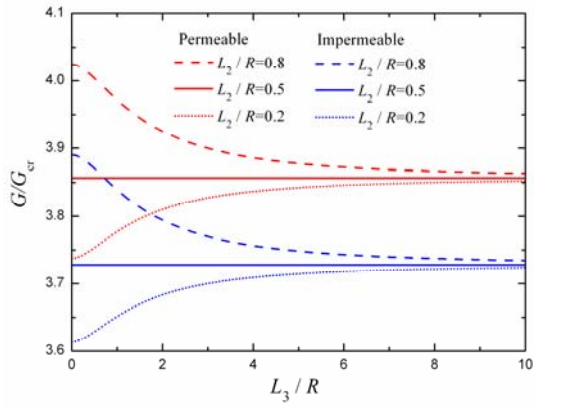

Fig. 4 Variation of G/G_{cr} with a ratio of L_3/R

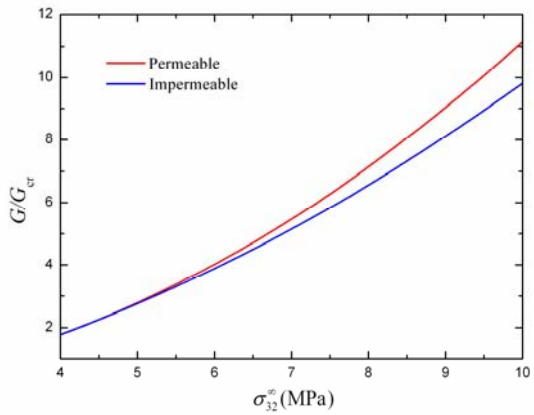

Fig. 5 Effect of applied mechanical loading on the normalized ERR

In what follows, to consider the effects of applied mechanical and electric loadings on the normalized ERR, we suppose a fixed-size hole of $R = 0.01\,\mathrm{m}$ and the cracks lengths $L_1 = 0.005\,\mathrm{m}$,

$L_2 = 0.008\,\mathrm{m}$ and $L_3 = 0.003\,\mathrm{m}$. Fig. 5 shows the influence of the applied mechanical loading on the normalized ERR under given electric load $D_2^{\infty} = 2\mathrm{e}-3\,\mathrm{C/m}^2$. As seen in the figure, the applied mechanical loading always promotes the crack growth, which is expectable. The effects of the applied electric load on the normalized ERR and the normalized MSERR are depicted under given mechanical loading $\sigma_{32}^{\infty} = 6\,\mathrm{MPa}$ in Figs. 6 and 7, respectively, where G_0^M denotes the value of the MSERR in the absence of remote electric load. It is seen from Figs. 6 and 7 that for the electrically permeable boundary condition, the normalized ERR and the MSERR are independent on the electric load, but dependent only on the mechanical loading. In other words, an applied electric field has no effect on the propagation of an electrically permeable case, which is in accordance with the results in Zhang and Gao [6]. As shown in Fig. 6, for the electrically impermeable case if a mechanical loading is applied, a negative electric load always decreases the normalized ERR, but a positive electric load either increases or decreases the normalized ERR. The result implies that a negative electric load is prone to retard the crack growth than a positive one. In contrast to Fig. 6, the positive electric field always increases the normalized MSERR, while the negative electric field always decreases the normalized MSERR in Fig. 7.

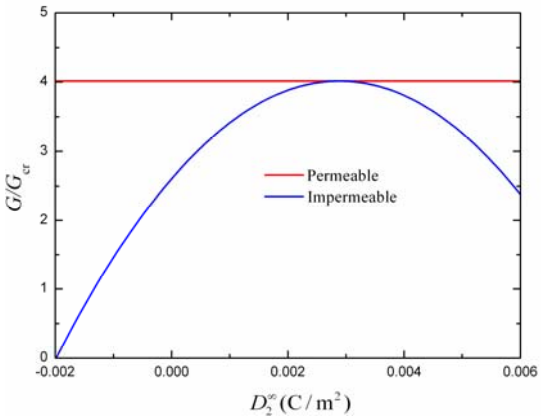

Fig. 6 Effect of applied electric loading on the normalized ERR

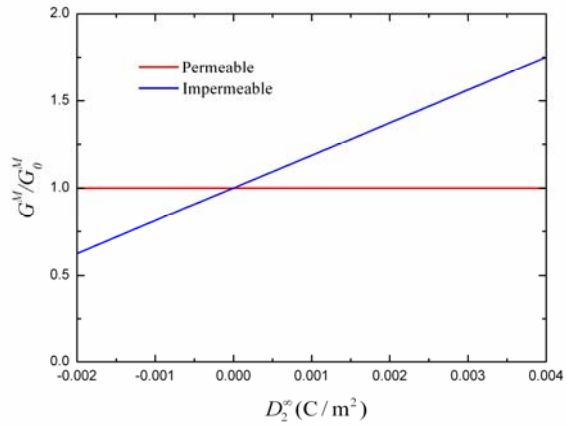

Fig. 7 Effect of applied electric loading on the normalized MSERR

6. Conclusions

The anti-plane problem of four non-symmetrical radial cracks at the edge of a circular hole in an infinite piezoelectric solid is investigated using the complex variable method and a new mapping function. This work is focused on the study of explicit and exact solutions in closed-form of the field intensity factors, ERR and MSERR. Several known results can be derived as special cases from the present solutions. Numerical results are provided to show the effects of geometrical parameters, applied mechanical and electric loads on ERR and MSERR. The results show that:

(a) The increase of the left crack length L_2 or right crack length L_1 always promotes the failure of piezoelectric materials for the case of four non-symmetric radial cracks at the edge of a circular hole.There are following three different results for the effects of the perpendicular crack on the

propagation of the horizontal crack. If the lengths of the left crack and the right crack originating from a circular hole are equal, an occurrence of the perpendicular cracks has no effect on the crack growth. If the length of left crack is larger than that of right crack, an increase of lengths of the perpendicular cracks can retard the crack growth. If the length of left crack is smaller than that of right crack, an increase of the length of the perpendicular cracks can promote the crack propagation.
(b) The electrically permeable boundary condition gives the highest value of ERR or MSERR, while the electrically impermeable case yields the lowest value of ERR or MSERR.
(c) The applied mechanical loading always promotes the crack growth, but the effects of applied electric fields on the crack growth depend on the different fracture parameters.

Acknowledgements

The authors thank the support from the National Natural Science Foundation of China (Nos.11262012 and 11262017), the Scientific Research Key Program of Inner Mongolia University of Technology (Grant No. ZD201219).

References

[1] Y.E. Pak, Crack extension force in a piezoelectric material, J Appl Mech, 57 (1990) 647– 653.
[2] Z. Suo, C. M. Kuo, D. M. Barnett, et al., Fracture Mechanics for Piezoelectric Ceramics, J Mech Phy Solids, 40 (1992) 739-765.
[3] H. Sosa, On the Fracture Mechanics of Piezoelectric Solids, Int J Solids Struct, 29 (1992) 2613-2622.
[4] W.T. Ang, L. Athanasius, A boundary integral approach for plane analysis of electrically semi-permeable planar cracks in a piezoelectric solid, Eng Analy Bound Elemen, 35 (2011) 647-656.
[5] C.Y. Fan, Y.F. Zhao, M.H. Zhao, E. Pan, Analytical solution of a semi-permeable crack in a 2D piezoelectric medium based on the PS model, Mech Res Commun, 40 (2012) 34-40.
[6] T.Y. Zhang, C.F. Gao, Fracture behaviors of piezoelectric materials, Theo Appl Fract Mech, 41 (2004) 339-379.
[7] Y.J. Wang, C.F. Gao, The mode III cracks originating from the edge of a circular hole in a piezoelectric solid, Int J Solids Struct, 45 (2008) 4590-4599.
[8] J.H. Guo, Z.X. Lu, H.T. Han, Z. Yang, Exact solutions for anti-plane problem of two asymmetrical edge cracks emanating from an elliptical hole in a piezoelectric material. Int J Solids Struct 46 (2009) 3799-3809.
[9] J.H. Guo, Z.X. Lu, H.T Han, Z. Yang, The behavior of two non-symmetrical permeable cracks emanating from an elliptical hole in a piezoelectric solid, Euro J Mech A/Solids, 29 (2010) 654-663.
[10] G.C. Sih, Stress distribution near internal crack tips for longitudinal shear problems, J Appl Mech, 32 (1965) 51.
[11] H. Tada, P.C. Paris, G.R. Irwin, The stress analysis of cracks handbook, Hellertown, PA: Del Research Corporation, 1973.
[12] T. Yokobori, M. Ichikawa, S. Konosu, R. Takahashi, A criterion for brittle fracture of notched solid, Japanese Society for strength and Fracture of Materials, 6 (1971) 58-67.